

## Systematic investigation on topological properties of layered GaS and GaSe under strain

Wei An, Feng Wu, Hong Jiang, Guang-Shan Tian, and Xin-Zheng Li

Citation: *The Journal of Chemical Physics* **141**, 084701 (2014); doi: 10.1063/1.4893346

View online: <http://dx.doi.org/10.1063/1.4893346>

View Table of Contents: <http://scitation.aip.org/content/aip/journal/jcp/141/8?ver=pdfcov>

Published by the [AIP Publishing](#)

---

### Articles you may be interested in

Structural, electronic, mechanical, and dynamical properties of graphene oxides: A first principles study  
*J. Appl. Phys.* **115**, 203517 (2014); 10.1063/1.4878938

Electronic properties of III-nitride semiconductors: A first-principles investigation using the Tran-Blaha modified Becke-Johnson potential  
*J. Appl. Phys.* **114**, 183702 (2013); 10.1063/1.4829674

DFT investigations of structural and electronic properties of gallium arsenide (GaAs)  
*AIP Conf. Proc.* **1482**, 64 (2012); 10.1063/1.4757439

First-principles investigations of Zn (Cd) doping effects on the electronic structure and magnetic properties of CoFe<sub>2</sub>O<sub>4</sub>  
*J. Appl. Phys.* **109**, 07A502 (2011); 10.1063/1.3535442

Optical properties of GaSe grown with an excess and a lack of Ga atoms  
*J. Appl. Phys.* **94**, 5399 (2003); 10.1063/1.1609045

---



# Systematic investigation on topological properties of layered GaS and GaSe under strain

Wei An,<sup>1</sup> Feng Wu,<sup>2</sup> Hong Jiang,<sup>2,a)</sup> Guang-Shan Tian,<sup>1</sup> and Xin-Zheng Li<sup>1,3,b)</sup>

<sup>1</sup>School of Physics, Peking University, Beijing 100871, People's Republic of China

<sup>2</sup>Beijing National Laboratory for Molecular Sciences, College of Chemistry and Molecular Engineering, Peking University, Beijing 100871, People's Republic of China

<sup>3</sup>Collaborative Innovation Center of Quantum Matter, Beijing 100871, People's Republic of China

(Received 19 May 2014; accepted 6 August 2014; published online 22 August 2014)

The topological properties of layered  $\beta$ -GaS and  $\epsilon$ -GaSe under strain are systematically investigated by *ab initio* calculations with the electronic exchange-correlation interactions treated beyond the generalized gradient approximation (GGA). Based on the *GW* method and the Tran-Blaha modified Becke-Johnson potential approach, we find that while  $\epsilon$ -GaSe can be strain-engineered to become a topological insulator,  $\beta$ -GaS remains a trivial one even under strong strain, which is different from the prediction based on GGA. The reliability of the fixed volume assumption rooted in nearly all the previous calculations is discussed. By comparing to strain calculations with optimized inter-layer distance, we find that the fixed volume assumption is qualitatively valid for  $\beta$ -GaS and  $\epsilon$ -GaSe, but there are quantitative differences between the results from the fixed volume treatment and those from more realistic treatments. This work indicates that it is risky to use theoretical approaches like GGA that suffer from the band gap problem to address physical properties, including, in particular, the topological nature of band structures, for which the band gap plays a crucial role. In the latter case, careful calibration against more reliable methods like the *GW* approach is strongly recommended.

© 2014 AIP Publishing LLC. [<http://dx.doi.org/10.1063/1.4893346>]

## I. INTRODUCTION

In recent years, topological insulators (TIs) have attracted much attention because of their intriguing physics and promising applications in electronic and spintronic devices.<sup>1–3</sup> Normally, TIs have a well-defined insulating gap in the bulk as conventional insulators and gapless surface states at the boundary. Consisting of an odd number of Dirac fermions and protected by the time-reversal symmetry, the TIs' surface states have no backscattering via transport and are quite robust against impurities. To distinguish a TI from a normal insulator, the standard recipe is to calculate its  $Z_2$  topological invariants in the bulk phase using the topological band theory.<sup>4</sup> As a rule of thumb, the spin-orbit coupling (SOC) induced band inversion at time-reversal-invariant momentum points of the Brillouin zone (BZ) can be used as an indicator. Lots of materials bearing a narrow gap and containing heavy elements (therefore large SOC effects) have been proposed to be TIs, such as  $\text{Bi}_2\text{Se}_3$  family,<sup>5</sup> thallium-based ternary III-V-VI<sub>2</sub> chalcogenides,<sup>6–10</sup> Pb-based ternary chalcogenides,<sup>11</sup> distorted bulk HgTe, and strained ternary Heusler compounds.<sup>12,13</sup>

In a recent work by Zhu *et al.*,<sup>14</sup> it has been further demonstrated that even materials comprised by light elements with rather weak SOC can be transformed to TIs under appropriate strain. The two examples used on proposing this idea are GaS and GaSe.<sup>15,16</sup> The electronic structures

of these two materials are highly anisotropic due to their layered structure composed of stacking of the X–Ga–Ga–X (X = S, Se) slabs with weak van der Waals (vdW) interactions. Among the existing different polytypes, the  $\beta$ -type structure with the space group  $P6_3/mmc$  (No. 194) is the most stable for GaS, while the  $\epsilon$ -type structure with the space group  $P\bar{6}m2$  (No. 187) is the most stable one for GaSe (see Figs. 1(a) and 1(b), respectively). Following the proposal by Zhu *et al.*,<sup>14</sup> new families of TIs have been predicted through strain engineering, such as  $\beta$ -InSe,<sup>17</sup>  $\text{TiTe}_2$ ,<sup>18</sup> and hexagonal wurtzite-type binary compounds AuI and AgI.<sup>19</sup> However, one needs to acknowledge that most of the theoretical predictions on TIs up to now are based on density-functional theory (DFT) calculations using the Perdew-Burke-Ernzerhof (PBE) generalized gradient approximation (GGA)<sup>20</sup> for the exchange-correlation functional, which often significantly underestimates band gaps in semiconductors and insulators.<sup>21,22</sup> It has been shown that there is significant discrepancy on the prediction of TI properties between more accurate *GW* calculations and the PBE ones.<sup>23,24</sup> Indeed, using the Tran-Blaha modified Becke-Johnson (TB-mBJ) potential method, which yields accurate band gaps comparable with the *GW* approach,<sup>25,26</sup> Huang *et al.*<sup>27</sup> have shown that  $\beta$ -GaS is a normal insulator even under 30% biaxial tension, in strong contrast to the PBE results. A more systematic reassessment of the topological property of both  $\beta$ -GaS and  $\epsilon$ -GaSe in which exchange-correlation interactions are treated beyond the PBE level is therefore highly desired. In addition, the strain calculations reported in previous studies are all based on the fixed-volume assumption<sup>23,27</sup> and

<sup>a)</sup>Electronic mail: h.jiang@pku.edu.cn

<sup>b)</sup>Electronic mail: xzli@pku.edu.cn

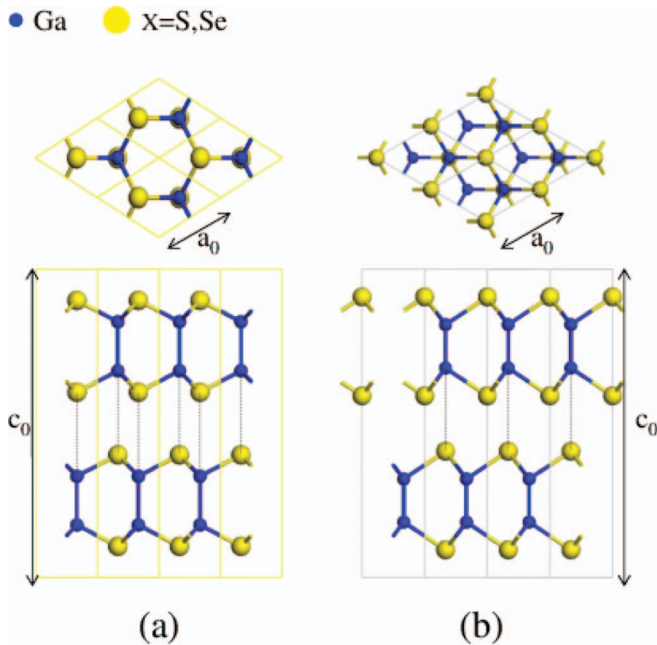


FIG. 1. Structures of the  $\beta$ - and  $\epsilon$ -phases in the GaS and GaSe systems. Panel (a) shows the top and side views of the  $\beta$ -phase. Panel (b) shows the top and side views of the  $\epsilon$ -phase.

whether it is reliable to layered GaS and GaSe also needs further scrutiny.

In this work, we systematically investigate the topological properties of layered  $\beta$ -GaS and  $\epsilon$ -GaSe under strain based on both the  $GW$  approach and the TB-mBJ method. The paper is organized as following. In Sec. II, we give a brief overview on theoretical approaches used in the study and present some computational details of our calculations. In Sec. III, we first make a careful comparison between different theoretical approaches, especially  $GW$  and TB-mBJ, on the description of electronic band structures of  $\beta$ -GaS and  $\epsilon$ -GaSe with unstrained experimental structures. Then we use the TB-mBJ method to investigate the evolution of the topological properties of  $\beta$ -GaS and  $\epsilon$ -GaSe under strain. Finally, the effects of the fixed volume assumption used in many strain-engineering studies are investigated by a more realistic treatment of biaxial strain. Section IV summarizes the main findings of the work.

## II. THEORY AND COMPUTATIONAL DETAILS

### A. Theoretical methods

The fundamental band gap of a material is often systematically underestimated by DFT with the LDA/GGA type exchange-correlation functionals.<sup>21,22</sup> Many-body perturbation theory in the  $GW$  approximation (GWA),<sup>28</sup> in which the quasi-particle (QP) self-energy  $\Sigma_{xc}$  is calculated as the product of one-body Green function  $G$  and the screened Coulomb interaction  $W$ , is currently the most accurate first-principles approach to describe electronic band structure of insulating systems.<sup>29</sup> In practice, the  $GW$  QP energies are often calculated as a first-order correction to LDA/GGA Kohn-Sham (KS) band energies, with both  $G$  and  $W$  calculated from

KS eigenenergies and eigenfunctions, hence termed as the  $G_0W_0$  approach. For simple semiconductors, the partially self-consistent  $GW$ , the so-called  $GW_0$  approach, in which  $G$  is re-calculated iteratively using QP energies with fixed  $W_0$ , can often give optimal performance without introducing much computational overhead.<sup>30–32</sup> To further get rid of the dependence on the KS reference required in  $G_0W_0$  and  $GW_0$ , several different approximate self-consistent  $GW$  (sc $GW$ ) approaches have also been proposed.<sup>33,34</sup> In practice, however, they tend to overestimate band gaps and therefore may not necessarily be an improvement compared to  $G_0W_0$  and  $GW_0$  in describing the band gaps of normal semiconductors and insulators.<sup>34</sup> In addition, they are computationally much more expensive and therefore not feasible for extensive calculations.

Considering the heavy computational cost of the  $GW$  approaches, in this work we also employ the recently proposed TB-mBJ approach, which uses a meta-GGA type exchange-correlation potential and is able to describe band gaps of many semiconductors surprisingly well.<sup>25,26,35</sup> In particular, we use the PBE-based perturbative TB-mBJ approach, which, as shown in our previous publication,<sup>26</sup> is both accurate and numerically stable on reproducing the band gaps of a variety of insulators and semiconductors with an accuracy comparable to that of the  $GW$  approach in many cases. The TB-mBJ approach has already been used to investigate the band topology in recent years and its predictive power has been verified by several previous works.<sup>12,27,36</sup> In particular, the band symmetry near the band edge which is essential for assigning the topological nature of the material can be well described by mBJ.<sup>37,38</sup>

The TB-mBJ approach can be regarded as a pragmatic approach to address the LDA/GGA band gap problem in the DFT framework. On the other hand, considering that the TB-mBJ potential depends on parameters that are empirically determined,<sup>25</sup> it is important, when studying new materials, to monitor its performances by comparing to more accurate treatments. In this work, we mainly use the TB-mBJ approach to investigate topological properties of GaS and GaSe under strain, and its accuracy is confirmed by the  $GW$  approaches for a few selected cases.

### B. Computational details

All DFT calculations, including LDA, PBE, and TB-mBJ ones, are performed using the WIEN2k package<sup>39</sup> in which the Kohn-Sham equations are solved in the full-potential linearized augmented plane-wave (FP-LAPW) basis. The following parameters are used for the LAPW basis: The muffin-tin (mt) radii  $R_{mt}$  are 2.2, 2.0, and 2.0 bohrs for Ga, S, and Se, respectively, and the plane wave cutoff is determined by setting  $\min R_{mt} K_{max} = 7$ . In all DFT calculations, we use a  $16 \times 16 \times 3$   $\mathbf{k}$ -mesh for the integration of the Brillouin zone. The SOC is considered based on the second-variational approach in which scalar relativistic orbitals up to 10 Ry above the Fermi level are considered.

For unstrained  $\beta$ -GaS and  $\epsilon$ -GaSe, the experimental lattice constants are used, namely,  $a = 3.587 \text{ \AA}$ ,  $c = 15.492 \text{ \AA}$  for

$\beta$ -GaS<sup>15</sup> and  $a = 3.752 \text{ \AA}$ ,  $c = 15.95 \text{ \AA}$  for  $\epsilon$ -GaSe.<sup>16</sup> Strain is applied by increasing the lattice constant  $a$  under the fixed volume assumption, i.e., the volume of the unit cell keeps constant under the strain.<sup>14</sup> Then for each strained structure, we optimize the internal atomic coordinates, using a force convergence tolerance of 0.5 mRy/bohr. When the fixed volume approximation is released, for each strained lattice constant of  $a$ , we monitor the evolution of the system's total energy as a function of  $c$ , so that the physical geometry of the system under biaxial strain can be obtained.

For  $G_0W_0$  and  $GW_0$  calculations, we use the LAPW-based all-electron  $GW$  code, FHI-gap,<sup>32</sup> which is interfaced to WIEN2k.<sup>39</sup> To ensure the convergence within 0.05 eV for the band gap, we consider 120 unoccupied bands and use a  $6 \times 6 \times 2$   $\mathbf{k}$ -mesh for the BZ integration. The SOC effect is considered in  $GW$  calculations perturbatively by using the scalar relativistic KS wavefunctions and  $GW$  quasi-particle energies as the input for a one-shot second variational calculation.<sup>40</sup> The  $GW$  band diagrams are obtained by using the Fourier interpolation approach.<sup>41</sup>

In a few cases, we also perform quasi-particle scGW calculations using the VASP code.<sup>34</sup> We use the PAW-PBE pseudopotential with the valence configurations of  $3d^{10}4s^24p^1$ ,  $3s^23p^4$ , and  $4s^24p^4$  for Ga, S, and Se, respectively. The plane wave energy cutoff is taken as 280 eV and a  $6 \times 6 \times 2$   $\mathbf{k}$ -mesh is used for the ground-state calculations. For the scGW calculations, the total number of bands, the plane wave cutoff energy for the evaluation of the polarization function and the number of frequency points are 150, 180 eV and 50, respectively. The scGW self-consistency threshold is 0.01 eV for the band gap at the  $\Gamma$  point.

### III. RESULTS

#### A. Comparison between the $GW$ approach and the mBJ method

We start our discussions from  $\beta$ -GaS and  $\epsilon$ -GaSe in unstrained experimental crystal structure, for which experimental band gaps are available. Fig. 2 shows the direct band gaps at the  $\Gamma$  point of the two unstrained structures obtained from different theoretical approaches compared to experiment. For the  $GW$  calculations, we used three different schemes, including: (i) PBE based  $G_0W_0$ , (ii) PBE based  $GW_0$ , and (iii) scGW. While  $G_0W_0$  and mBJ slightly underestimate these band gaps, scGW seriously overestimates these values by  $\sim 1$  eV. Among all the schemes, the PBE based  $GW_0$  method presents the best agreement with experiment.<sup>42</sup>

More complete results on the band gaps of unstrained  $\beta$ -GaS and  $\epsilon$ -GaSe are collected in Table I. As expected, the consideration of SOC has little effects on the band gaps of GaS, and only reduces the band gaps of  $\epsilon$ -GaSe by about 0.03 eV. Our PBE calculations reproduce the results of Ref. 14 that  $\beta$ -GaS has an indirect fundamental gap from M to  $\Gamma$  and  $\epsilon$ -GaSe has a direct fundamental gap at the  $\Gamma$  point. Though the indirect band gap feature in  $\beta$ -GaS is reproduced by PBE compared with experiment,<sup>42</sup> this value is underestimated by more than 1 eV (1.580 eV compared with 2.591 eV). For  $\epsilon$ -GaSe, PBE predicts a direct fundamental

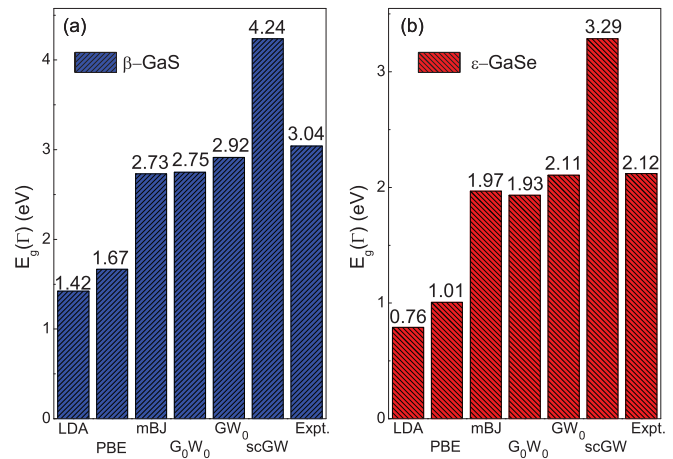


FIG. 2. The direct band gap (in units of eV) at the  $\Gamma$  point ( $\mathbf{k} = 0$ ) obtained from different theoretical methods and experiment (Ref. 42) for unstrained  $\beta$ -GaS (a) and  $\epsilon$ -GaSe (b), respectively.

band gap of 1.032 eV, which is even qualitatively wrong compared with the indirect band gap observed in experiment. And again, both the  $\Gamma$ -M and  $\Gamma$ - $\Gamma$  band gap are underestimated by about 1 eV. It is interesting to note that LDA gives even smaller band gaps than PBE for both  $\beta$ -GaS and  $\epsilon$ -GaSe, and in both cases the fundamental gap is predicted wrongly to be direct. Very good agreement with experiment is obtained by  $GW_0$ , which predicts accurate indirect fundamental band gaps for both  $\beta$ -GaS and  $\epsilon$ -GaSe. Overall the mBJ approach gives results that are very close to those of  $GW_0$ , except that it still predicts  $\epsilon$ -GaSe to have an indirect fundamental gap, but the difference between  $\Gamma$ - $\Gamma$  and  $\Gamma$ -M gaps is significantly smaller than that from the PBE prediction.

Figure 3 shows the band structure diagrams of unstrained  $\beta$ -GaS and  $\epsilon$ -GaSe from different theoretical approaches. The band dispersion of LDA and PBE are very similar such that the latter can be nearly obtained by a 0.2 eV rigid shift for all  $\mathbf{k}$ -points in BZ from the former. The  $GW$  correction to the conduction band bottom at  $\Gamma$  is significantly larger than that at M, which enhances the indirect band gap feature in both systems. In  $\beta$ -GaS, the lowest conduction band energies at M and  $\Gamma$  are close at the PBE level, with that at M slightly lower. Therefore, this vaguely correct feature at the PBE level is

TABLE I. The  $\Gamma$ - $\Gamma$  and  $\Gamma$ -M band gap for unstrained  $\beta$ -GaS and  $\epsilon$ -GaSe using LDA, PBE,  $GW_0$ , and mBJ method with and without SOC.

	$\beta$ -GaS		$\epsilon$ -GaSe	
	$\Gamma$ - $\Gamma$	$\Gamma$ -M	$\Gamma$ - $\Gamma$	$\Gamma$ -M
LDA	1.422 <sup>a</sup>	1.432	0.790 <sup>a</sup>	1.171
LDA+SOC	1.421 <sup>a</sup>	1.430	0.764 <sup>a</sup>	1.140
PBE	1.667	1.580 <sup>a</sup>	1.032 <sup>a</sup>	1.341
PBE+SOC	1.667	1.580 <sup>a</sup>	1.007 <sup>a</sup>	1.312
$GW_0$	2.915	2.423 <sup>a</sup>	2.131	2.080 <sup>a</sup>
$GW_0$ +SOC	2.913	2.421 <sup>a</sup>	2.106	2.049 <sup>a</sup>
mBJ	2.731	2.307 <sup>a</sup>	1.987 <sup>a</sup>	2.041
mBJ+SOC	2.730	2.306 <sup>a</sup>	1.968 <sup>a</sup>	2.019
Expt. (Ref. 42)	3.040	2.591 <sup>a</sup>	2.120	2.065 <sup>a</sup>

<sup>a</sup>Fundamental gap.

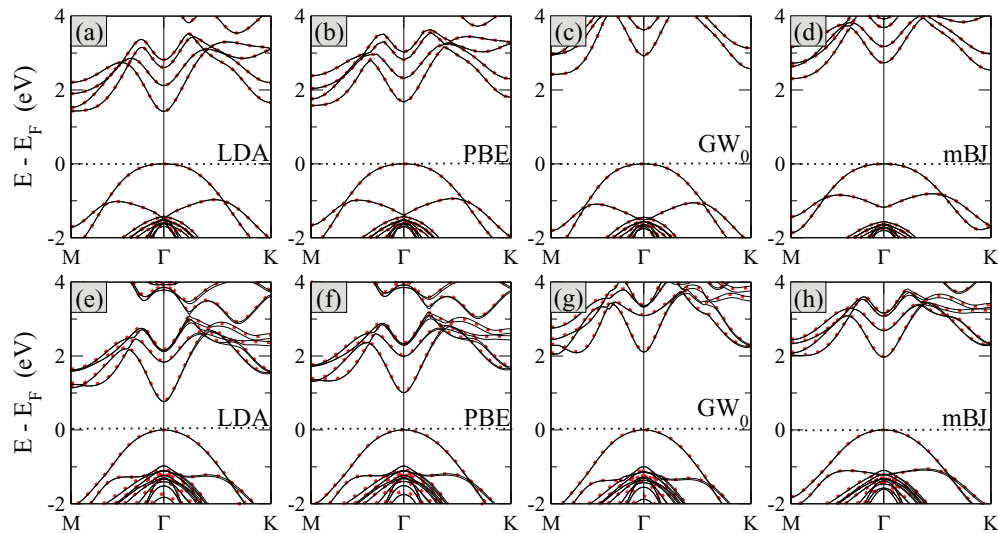


FIG. 3. Band diagrams of  $\beta$ -GaS (upper panels) and  $\epsilon$ -GaSe (lower panels) from the LDA (a) and (e), PBE (b) and (f),  $GW_0$  (c) and (g), and one-shot mBJ (d) and (h) calculations. The black solid (red dotted) lines correspond to calculations with (without) SOC effects.

obviously enhanced when the  $GW$  correction is applied. For  $\epsilon$ -GaSe, at the PBE level, the lowest conduction band energy at M is significantly higher than that at  $\Gamma$ , which is corrected by  $GW$ . As shown in the right column of Fig. 3, the mBJ band diagram can reproduce the main features of the  $GW_0$  results. There are some noticeable differences in the dispersion of the second highest valence band in  $GW_0$  and mBJ band diagrams of  $\beta$ -GaS, which is possibly due to the general tendency of the mBJ approach to underestimate the valence band width.<sup>43</sup>

We further compare the results from  $GW_0$  and mBJ in band structure calculations for a few strained structures. The evolution of the  $\Gamma$  point band gap as a function of strain is shown in Fig. 4. We have mentioned that the  $GW_0$  approach is intrinsically a perturbation method whose performances depend on the quality of the starting point, i.e., PBE KS single-particle states in our case. Therefore, we only use the  $GW_0$  approach to the small strain cases ( $a/a_0 < 1.04$ ) where the PBE KS results can be regarded as qualitatively correct starting point. Fig. 4 shows that the mBJ method presents almost identical results with the  $GW_0$  approach for both  $\beta$ -GaS and  $\epsilon$ -GaSe under small strain. Therefore, we can use this  $GW$  justified mBJ approach to study the evolution

of the electronic structure under strain over the whole strain range.

## B. Topological property of $\beta$ -GaS and $\epsilon$ -GaSe via strain engineering

We first discuss the results on the topological property of  $\beta$ -GaS. The evolution of the  $\Gamma$  point band gap ( $E_g(\Gamma)$ ) with the biaxial strain is shown in Fig. 4(a). According to Zhu *et al.*,<sup>14</sup> the band inversion (negative  $E_g(\Gamma)$ ) implies a topologically nontrivial phase. As for the unstrained structure, the LDA results are still quite similar to the PBE ones for all the strained structures except for a rigid shift of about 0.2 eV, and therefore the topological properties predicted by LDA and PBE are essentially the same. In the PBE calculations, a topological phase transition from a normal insulator to a topological insulator can be observed at  $a/a_0 \sim 1.06$ .  $E_g(\Gamma)$  decreases continuously all the way to  $a/a_0$  equals 1.12, leading to the conclusion that  $\beta$ -GaS is a TI under appropriate strain. When the applied strain is larger than 12%,  $E_g(\Gamma)$  starts to increase and become positive at  $a/a_0 > 1.18$ , indicating the recovery of the normal insulating phase. Therefore, for  $\beta$ -GaS, two topological phase transitions should occur with increasing biaxial

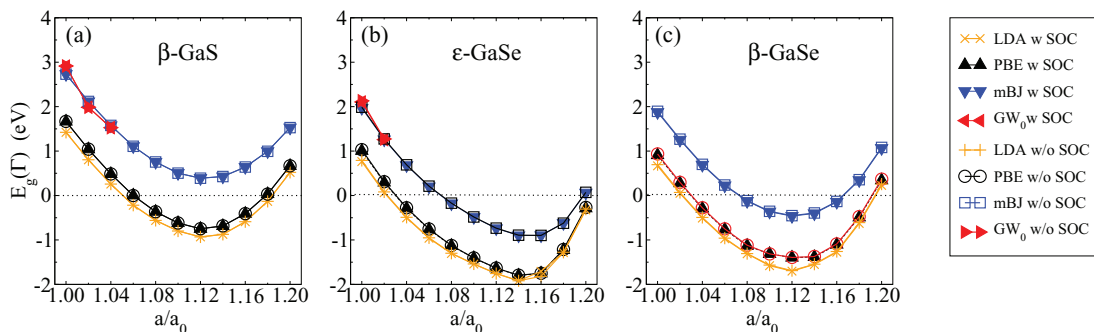


FIG. 4. Evolution of the direct band gap with strain in (a)  $\beta$ -GaS, (b)  $\epsilon$ -GaSe, (c) and  $\beta$ -GaSe. Different methods were used. The strain is characterized by  $a/a_0$ , where  $a_0$  represents the in-plane lattice constant without strain while the  $a$  represents the one with strain.

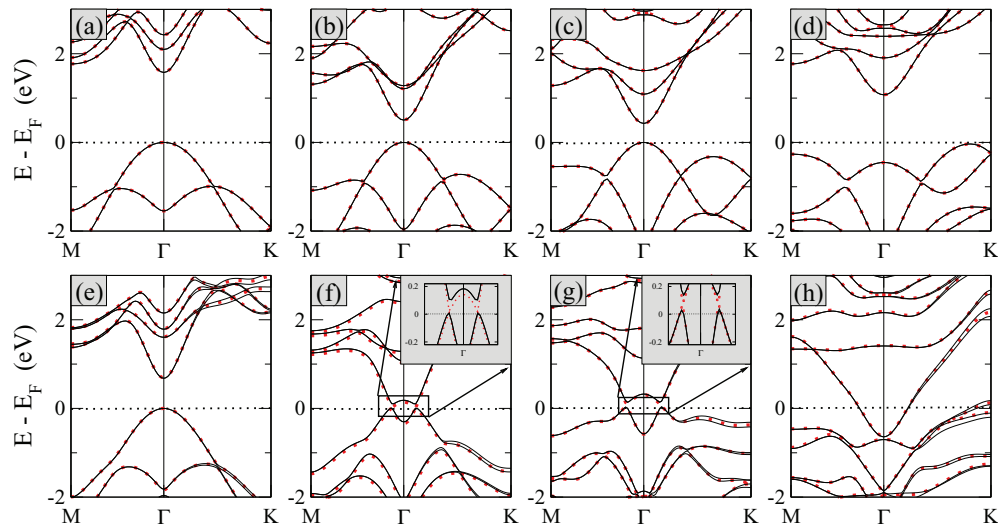


FIG. 5. Band diagrams of  $\beta$ -GaS (a)–(d) and  $\epsilon$ -GaSe (e)–(h) at  $ala_0$  equals 1.04, 1.1, 1.14, and 1.2 obtained using one-shot mBJ. The black solid (red dotted) lines correspond to calculations with (without) SOC effects. The inset in (f) and (g) shows the details around the Fermi level.

strain according to the PBE predicted band structures within the fixed volume approximation.

The results given by the mBJ approach are very different. An opening of  $E_g(\Gamma)$  compared to the PBE results is observed all the way from  $ala_0 = 1$  to  $ala_0 = 1.20$ , and most importantly  $E_g(\Gamma)$  remains positive for all strained structures studied. This difference indicates that the band inversion as predicted by the PBE calculations disappears upon treating the band gap problem more accurately. The absence of the band inversion can be further demonstrated by the evolution of band diagram with respect to strain for  $\beta$ -GaS, as shown by the upper panels of Fig. 5. Therefore,  $\beta$ -GaS under strain is still a trivial insulator instead of a TI based on the prediction of the mBJ approach.

Now we consider the second material, i.e.,  $\epsilon$ -GaSe. As shown in Fig. 4(b) and the lower panels in Fig. 5,  $E_g(\Gamma)$  in  $\epsilon$ -GaSe evolves as a function of strain in a similar way as in  $\beta$ -GaS: it first decreases, reaches a minimum at certain strain, and then increases. The band inversion occurs at  $ala_0$  around 1.03 in the PBE calculations. Using the mBJ method, although an opening of  $E_g(\Gamma)$  in comparison with PBE is still present for all strains studied, the band inversion still happens for  $1.07 \lesssim ala_0 \lesssim 1.2$ , indicating that  $\epsilon$ -GaSe might undergo a phase transition from a normal insulator to a TI with increasing biaxial strain. However, due to the fact that  $\epsilon$ -GaSe has no inversion symmetry, the band inversion itself is not sufficient to identify such a topological transition and a full evaluation of the  $Z_2$  topological invariants is required to determine its topological nature.<sup>4,44</sup> One method to circumvent this problem is to investigate an adiabatic transformation from  $\epsilon$ -GaSe to  $\beta$ -GaSe.<sup>14</sup> For the latter material, which has the inversion symmetry, a band inversion will be sufficient to identify its topological state. If a continuous connection between  $\epsilon$ -GaSe and  $\beta$ -GaSe exists, the former material's topological feature can then be confirmed.

Based on the consideration above, we further performed similar calculations for  $\beta$ -GaSe, and the results are shown in Fig. 4(c). The unstrained structure of  $\beta$ -GaSe is obtained from

experiment.<sup>16</sup> Similar to  $\epsilon$ -GaSe, although the mBJ method gives rise to larger  $E_g(\Gamma)$  compared to LDA and PBE, a band inversion still occurs at  $ala_0 \sim 1.08$ . To assign the topological order of  $\epsilon$ -GaSe, an adiabatic connection between  $\epsilon$ -GaSe and  $\beta$ -GaSe is built at the strain  $ala_0 = 1.08$ . We strictly follow the transformation route proposed by Zhu *et al.*,<sup>14</sup> i.e.,  $\epsilon$ -GaSe  $\rightarrow$   $\epsilon'$ -GaSe  $\rightarrow$   $o$ -GaSe  $\rightarrow$   $\beta$ -GaSe. As shown in Fig. 6, the band structures near the Fermi level exhibit little change along the transformation path, which indicates that  $\epsilon$ -GaSe shares the same topological order with  $\beta$ -GaSe at the strain of  $ala_0 = 1.08$ . Similar analysis can be easily generalized to other strained structures. Therefore, it is confirmed that  $\epsilon$ -GaSe can be transformed to a topological insulator by imposing appropriate biaxial strain, when the electronic interactions are addressed by mBJ and the fixed volume approximation is used.

Releasing of the fixed volume approximation will be discussed in Sec. III C. Before going there, it is also worth

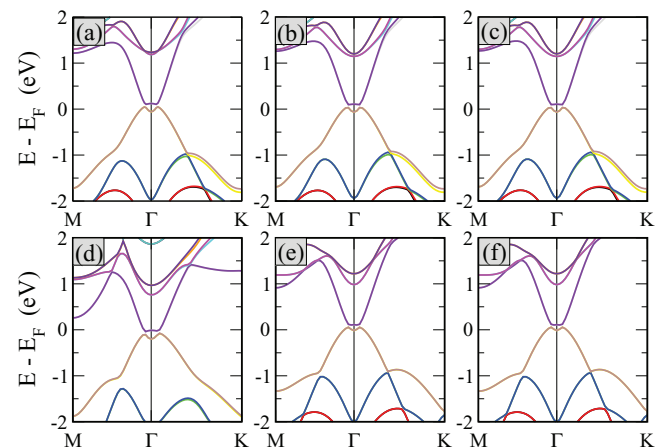


FIG. 6. Fully relativistic electronic band structures of (a)  $\epsilon$ -GaSe, (b) hypothetical  $\epsilon'$ -GaSe, (c)–(e) hypothetical  $o$ -GaSe with  $d = 0.0001d_0$ ,  $d = 0.5d_0$ , and  $d = 0.9999d_0$ , respectively, and (f)  $\beta$ -GaSe. See Ref. 14 for the definition of  $d_0$ .

mentioning that the SOC correction is rather weak and can be ignored for almost all results discussed above. This can be easily seen in Fig. 4, where it is clear that there is nearly no difference in description of the evolution of  $E_g(\Gamma)$  with strain between calculations with and without SOC effects. Detailed values for the band gaps in calculations of both materials under no strain are given in Table I.  $\beta$ -GaS contains only light elements, therefore, the SOC effects are smaller than 2 meV for all values shown. In  $\epsilon$ -GaSe, these effects are larger due to the heavier mass of Se. However, it is still clear from Fig. 4 that strain, instead of the SOC, is the dominant issue for the closing of the band gaps. Besides these, it is also obvious in Figs. 3 and 5 that the band dispersions obtained by different methods (LDA, PBE, mBJ, and  $GW_0$ ) for both  $\beta$ -GaS and  $\epsilon$ -GaSe are almost the same with and without SOC effect. The only exception is that the degeneracy of eigenvalue is absent due to the SOC interaction, such as the inset of (f) and (g) in Fig. 5. With these, we conclude that all the band inversion observed by now is ascribed to strain rather than the SOC effect, however, the SOC is responsible for the opening of a small gap at the degenerate  $k$ -points when band inversion occurred which is essential for TI's property. We note that this analysis is consistent with Refs. 14, 17 that for crystals with weak SOC effect appropriate strain might help to generate TIs.

### C. Releasing the fixed volume assumption

In Ref. 14, it was shown that if the strain is purely in-plane and the inter-layer distance is kept constant, the band inversion in  $\beta$ -GaS is deferred to  $ala_0 \sim 1.12$  and a monotonous decrease of the  $E_g(\Gamma)$  exists till  $ala_0$  equals 1.25 in the PBE calculations. Strains with fixed volume and fixed interlayer distance represent two very different scenarios. In the former case, as the inter-layer distance decreases, the dominant inter-layer interactions evolve from van der Waals interactions to covalent chemical bonding, while for the latter case van der Waals interactions are always dominant. We expect that a more realistic modeling of the biaxial strain is given by relaxing the inter-layer structures when the strain is imposed. In this section, we evaluate the adequacy of the fixed volume assumption by making a comparison to the results from more realistic calculations.

To calculate optimized inter-layer structures accurately, we first investigate the performances of different functionals, including LDA, PBE, PBEsol (PBE for solids),<sup>45</sup> and different variants of density-functional vdW methods (revPBE-vdW, rPW86-vdW2, optPBE-vdW, optB88-vdW, and optB88b-vdW),<sup>46</sup> in describing the equilibrium structures of  $\beta$ -GaS,  $\epsilon$ -GaSe, and  $\beta$ -GaSe.<sup>15,16</sup> Fig. 7 shows the relative error (RE) with respect to experimental results on the lattice parameters  $a$  and  $c$  for these structures calculated by different functionals. For the intralayer lattice parameter  $a$ , as usual, PBE overestimates and LDA underestimates it. The results of different vdW functionals do not show much improvement, and the best approximate functional for the description of the lattice parameter  $a$  is the PBEsol functional. However, what is more important is the accuracy of describing the inter-layer distance, i.e., the lattice parameter  $c$ . PBE and PBEsol overes-

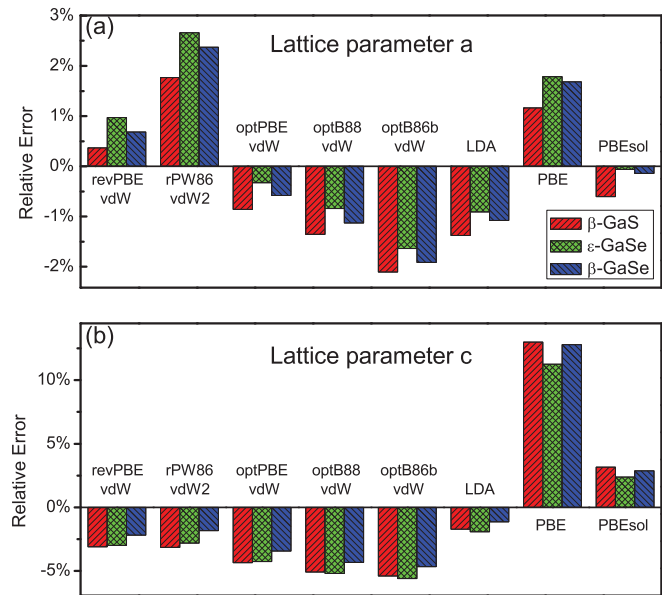


FIG. 7. The relative error (RE) of the lattice parameter  $a$  (a) and  $c$  (b) of  $\beta$ -GaS,  $\epsilon$ -GaSe, and  $\beta$ -GaSe with respect to experiment by different functionals.

timate it by 10% and 2.5%, respectively. All vdW functionals tend to underestimate  $c$  significantly, with a large RE around  $-4\%$  compared with that of LDA whose RE is only  $\sim -1\%$ . Therefore, our numerical analysis shows that LDA is most accurate as far as the description of inter-layer distance of GaX ( $X = S, Se$ ) is concerned, and therefore will be used for more realistic modeling of biaxial strain in the following.

We perform a series of full optimization calculations using different  $c$  at each  $a$  corresponding to a specific in-plane tension strain. Fig. 8 shows the total energy as a function of  $c$  for different in-plane strains. In  $\beta$ -GaS, at strain lower than  $ala_0 \sim 1.12$ , the minimum of the total energy curve is rather shallow (0.3 eV) at  $c$  around 13–15 Å, indicating that the inter-layer interactions are van der Waals-like. Further increasing biaxial tension beyond 12%, the binding energy suddenly becomes rather large ( $\sim 2.5$  eV). Meanwhile, the optimized  $c$  suddenly drops to about 10–11 Å. This abrupt change indicates that a discontinuous structural change happens at  $ala_0 \sim 1.12$  in more realistic simulations of the biaxial strain. Associated with this structural change, the inter-layer interactions evolve from being van der Waals-like to covalent chemical bonding.<sup>27</sup> To characterize the reliability of the fixed volume assumption at a quantitative level, we take the optimized value of the lattice constant  $c$  at each  $ala_0$  from Fig. 8 and compare them with the results obtained using the fixed volume approximation in Fig. 9. In the process of imposing biaxial strain ( $ala_0$  going from 1.00 to 1.20) in  $\beta$ -GaS, the evolution of the lattice constant  $c$  in the realistic simulation experiences a clear abrupt transition at  $ala_0 \simeq 1.12$ , in contrast to the smooth decreasing of  $c$  in the fixed-volume approximation. In the case of  $\epsilon$ -GaSe, Fig. 8(b) shows that the inter-layer binding energy continuously changes from  $\sim 0.1$  eV to  $\sim 1$  eV when  $ala_0$  goes from 1.00 to 1.20, and in the meanwhile the optimized  $c$  also changes smoothly from 15.5 Å to 11.5 Å.

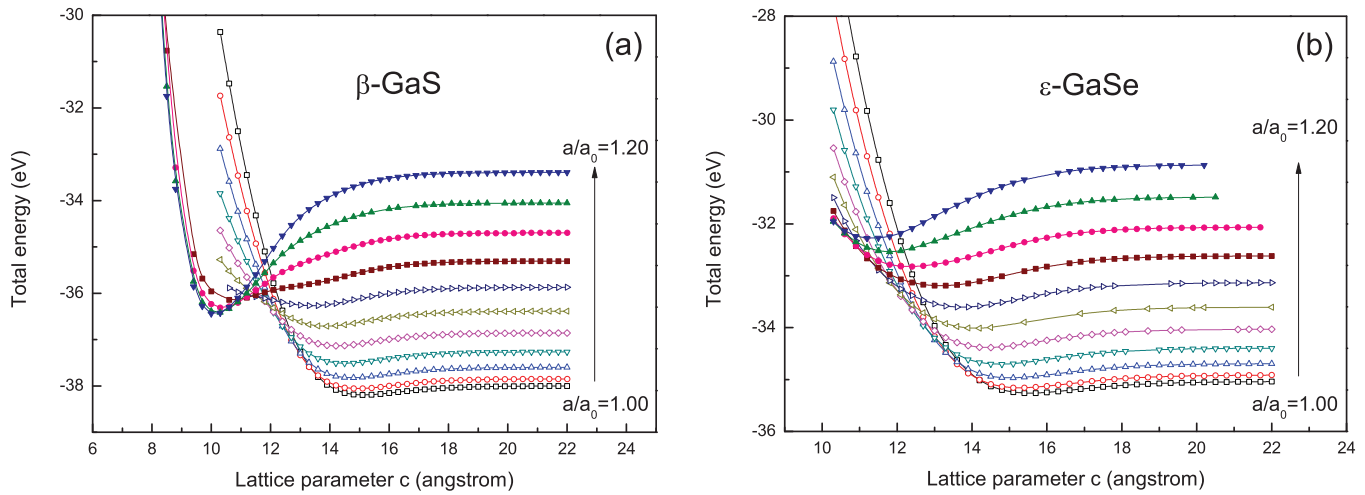


FIG. 8. The total energy as a function of the lattice parameter  $c$  at each in-plane biaxial tension for (a)  $\beta$ -GaS and (b)  $\epsilon$ -GaSe.

We can see that the optimized  $c$  differs quite significantly from that obtained from the fixed volume approximation. It is therefore important to know the effects of relaxing the fixed volume assumption on the band gaps of strained structures. Fig. 10 shows  $E_g(\Gamma)$  from mBJ as a function of strain with optimized and fixed-volume  $c$ , respectively. In general, the results from the two treatments are qualitatively similar. In particular, they predict the same topological phase transition behaviors based on the mBJ calculations that  $\beta$ -GaS remains a normal insulator under strain, and  $\epsilon$ -GaSe becomes a topological insulator within a certain range of strain. However, there are noticeable quantitative differences between two sets of results, and  $E_g(\Gamma)$  from using the optimized  $c$  changes in a more complicated way than that from using fixed-volume  $c$ , especially for  $\beta$ -GaS, which is consistent with the more dramatic change of  $c_{\text{opt}}$  in the former case. More importantly, the predicted critical strain ( $a^*/a_0$ ) at which the normal-to-topological phase transition occurs in  $\epsilon$ -GaSe is different: the fixed volume treatment predicts  $a^*/a_0 \simeq 1.07$ , but using  $c_{\text{opt}}$  gives  $a^*/a_0 \simeq 1.09$ . Our investigations

therefore indicate that the fixed-volume assumption is in general valid when studying topological insulators under strain, but more realistic treatments are required for a quantitative evaluation.

We close this section by noticing a few technical difficulties on practically using strain-engineering to convert  $\epsilon$ -GaSe to a topological insulator. We can see that the critical point of topological phase transition of  $\epsilon$ -GaSe predicted by TB-mBJ is actually quite challenging to reach in experiment. Normally, the biaxial strain is applied by growing sample on a lattice mismatched substrate.<sup>47</sup> Since the weak van der Waals interactions in layered structures reduce the bonding between the sample and the substrate, the strain induced in this way is only about 3%.<sup>48,49</sup> Even though large strain around 20% can be obtained in some rare cases,<sup>50</sup> it is often localized at the atomic scale and could impede electron transport. Therefore, new experimental techniques may be needed to achieve the strong biaxial strain to observe the normal-to-topological transition in  $\epsilon$ -GaSe.

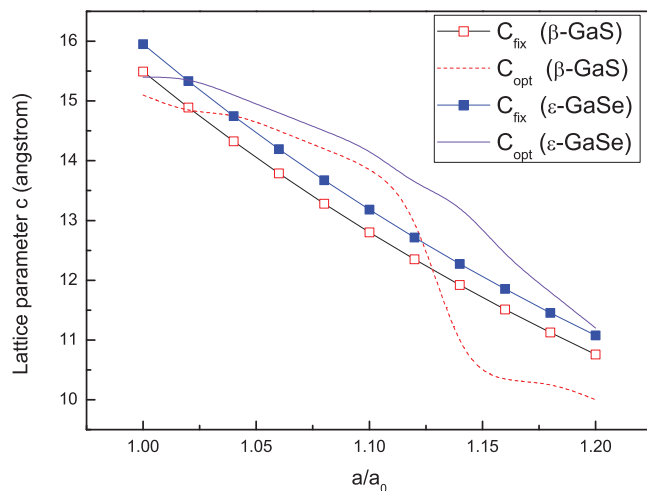


FIG. 9. The lattice parameter  $c$  as a function of biaxial strain for both  $\beta$ -GaS and  $\epsilon$ -GaSe, with volume fixed ( $C_{\text{fix}}$ ) and relaxed ( $C_{\text{opt}}$ ).

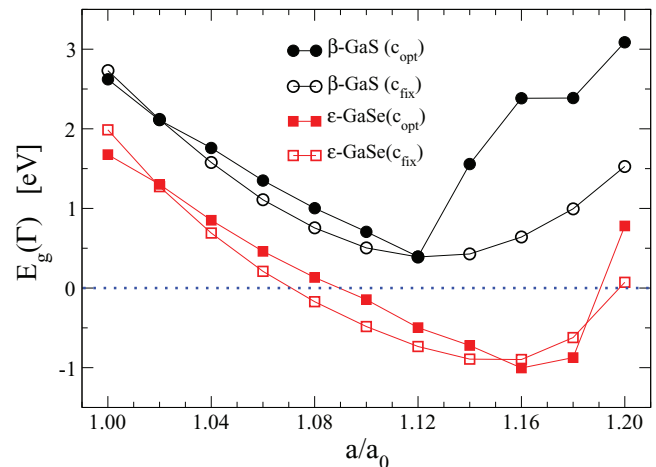


FIG. 10. Evolution of the direct band gap, calculated by the TB-mBJ approach, at the  $\Gamma$  point ( $E_g(\Gamma)$ ) with strain in  $\beta$ -GaS and  $\epsilon$ -GaSe with optimized  $c$  ( $c_{\text{opt}}$ ) and fixed-volume  $c$  ( $c_{\text{fix}}$ ).



#### IV. CONCLUSION

In summary, we systematically investigated the evolution of the topological feature of  $\beta$ -GaS and  $\epsilon$ -GaSe under strain. The influences of the often-used PBE functional and the fixed volume assumption in the description of such phenomena in previous studies are thoroughly analyzed. Based on more accurate treatment of electronic band structures by the *GW* and TB-mBJ approach, we show that while  $\epsilon$ -GaSe can be transformed to a topological insulator under certain strain,  $\beta$ -GaS remains a trivial one, which is different from the prediction based on PBE. Concerning the impact of the fixed volume approximation, we demonstrate that it is an appropriate approximation for both  $\beta$ -GaS and  $\epsilon$ -GaSe under strain qualitatively, but there are quantitative differences between the results from the fixed-volume treatment and those from more realistic treatment. Our study indicates the risk of using an approach like PBE-GGA to address physical properties, including, in particular, the topological nature of band structures, for which the band gap plays a crucial role. In the latter case, more careful calibration against the *GW* approach or other more reliable DFT methods is strongly recommended.

#### ACKNOWLEDGMENTS

This work is partly supported by the National Basic Research Programs of China under Grant No. 2013CB934600, the National Science Foundation of China (NSFC) under Grant Nos. 21173005, 21373017, 11374017, and 11275008, and the Open-Lab program (Project No. 12ZS01) of the Key Laboratory of Nanodevices and Applications, Suzhou Institute of Nano-Tech and Nano-Bionics (SINANO), Chinese Academy of Sciences (CAS). We thank Professor Yuguang Yao for helpful discussions. The computational resources were provided by the supercomputer TianHe-1A in Tianjin, China.

<sup>1</sup>J. E. Moore, *Nature (London)* **464**, 194 (2010).

<sup>2</sup>X.-L. Qi and S.-C. Zhang, *Rev. Mod. Phys.* **83**, 1057 (2011).

<sup>3</sup>M. Z. Hasan and C. L. Kane, *Rev. Mod. Phys.* **82**, 3045 (2010).

<sup>4</sup>L. Fu and C. L. Kane, *Phys. Rev. B* **76**, 045302 (2007).

<sup>5</sup>H. Zhang *et al.*, *Nat. Phys.* **5**, 438 (2009).

<sup>6</sup>H. Lin *et al.*, *Phys. Rev. Lett.* **105**, 036404 (2010).

<sup>7</sup>B. Yan *et al.*, *Europhys. Lett.* **90**, 37002 (2010).

<sup>8</sup>K. Kuroda *et al.*, *Phys. Rev. Lett.* **105**, 146801 (2010).

<sup>9</sup>Y. L. Chen *et al.*, *Phys. Rev. Lett.* **105**, 266401 (2010).

<sup>10</sup>T. Sato *et al.*, *Phys. Rev. Lett.* **105**, 136802 (2010).

<sup>11</sup>H. Jin, J.-H. Song, A. J. Freeman, and M. G. Kanatzidis, *Phys. Rev. B* **83**, 041202 (2011).

<sup>12</sup>W. Feng, D. Xiao, J. Ding, and Y. Yao, *Phys. Rev. Lett.* **106**, 016402 (2011).

<sup>13</sup>D. Xiao *et al.*, *Phys. Rev. Lett.* **105**, 096404 (2010).

<sup>14</sup>Z. Zhu, Y. Cheng, and U. Schwingenschlöggl, *Phys. Rev. Lett.* **108**, 266805 (2012).

<sup>15</sup>A. Kuhn, A. Chevy, and R. Chevalier, *Acta Crystallogr. B* **32**, 983 (1976).

<sup>16</sup>A. Kuhn, A. Chevy, and R. Chevalier, *Phys. Status Solidi B* **31**, 469 (1975).

<sup>17</sup>Y. Ma *et al.*, *New J. Phys.* **15**, 073008 (2013).

<sup>18</sup>Q. Zhang, Y. Cheng, and U. Schwingenschlöggl, *Phys. Rev. B* **88**, 155317 (2013).

<sup>19</sup>X. M. Zhang *et al.*, *Europhys. Lett.* **103**, 57012 (2013).

<sup>20</sup>J. P. Perdew, K. Burke, and M. Ernzerhof, *Phys. Rev. Lett.* **77**, 3865 (1996).

<sup>21</sup>J. P. Perdew and M. Levy, *Phys. Rev. Lett.* **51**, 1884 (1983).

<sup>22</sup>L. J. Sham and M. Schlüter, *Phys. Rev. Lett.* **51**, 1888 (1983).

<sup>23</sup>J. Vidal *et al.*, *Phys. Rev. B* **84**, 041109(R) (2011).

<sup>24</sup>O. V. Yazyev, E. Kioupakis, J. E. Moore, and S. G. Louie, *Phys. Rev. B* **85**, 161101 (2012).

<sup>25</sup>F. Tran and P. Blaha, *Phys. Rev. Lett.* **102**, 226401 (2009).

<sup>26</sup>H. Jiang, *J. Chem. Phys.* **138**, 134115 (2013).

<sup>27</sup>X. Huang *et al.*, *Phys. Rev. B* **88**, 235301 (2013).

<sup>28</sup>L. Hedin, *Phys. Rev.* **139**, A796 (1965).

<sup>29</sup>F. Aryasetiawan and O. Gunnarsson, *Rep. Prog. Phys.* **61**, 237 (1998).

<sup>30</sup>M. Shishkin and G. Kresse, *Phys. Rev. B* **75**, 235102 (2007).

<sup>31</sup>H. Jiang, R. Gomez-Abal, P. Rinke, and M. Scheffler, *Phys. Rev. B* **81**, 085119 (2010).

<sup>32</sup>H. Jiang *et al.*, *Comput. Phys. Commun.* **184**, 348 (2013).

<sup>33</sup>S. V. Faleev, M. van Schilfgaarde, and T. Kotani, *Phys. Rev. Lett.* **93**, 126406 (2004).

<sup>34</sup>M. Shishkin, M. Marsman, and G. Kresse, *Phys. Rev. Lett.* **99**, 246403 (2007).

<sup>35</sup>A. D. Becke and E. R. Johnson, *J. Chem. Phys.* **124**, 221101 (2006).

<sup>36</sup>Z. Zhu, Y. Cheng, and U. Schwingenschlöggl, *Phys. Rev. B* **85**, 235401 (2012).

<sup>37</sup>W. Feng, D. Xiao, Y. Zhang, and Y. Yao, *Phys. Rev. B* **82**, 235121 (2010).

<sup>38</sup>W. Feng and Y. Yao, *Sci. China Phys. Mech.* **55**, 2199 (2012).

<sup>39</sup>P. Blaha *et al.*, *WIEN2k, An Augmented Plane Wave Plus Local Orbitals Program for Calculating Crystal Properties* (Karlheinz Schwarz, Technical University of Vienna, Vienna, 2001).

<sup>40</sup>H. Jiang, *J. Chem. Phys.* **134**, 204705 (2011).

<sup>41</sup>W. E. Pickett, H. Krakauer, and P. B. Allen, *Phys. Rev. B* **38**, 2721 (1988).

<sup>42</sup>E. Aulich, J. L. Brebner, and E. Mooser, *Phys. Status Solidi B* **31**, 129 (1969).

<sup>43</sup>D. Waroquiers *et al.*, *Phys. Rev. B* **87**, 075121 (2013).

<sup>44</sup>W. Feng *et al.*, *Comput. Phys. Commun.* **183**, 1849 (2012).

<sup>45</sup>J. P. Perdew *et al.*, *Phys. Rev. Lett.* **100**, 136406 (2008).

<sup>46</sup>J. Klimeš, D. R. Bowler, and A. Michaelides, *Phys. Rev. B* **83**, 195131 (2011).

<sup>47</sup>F. Guinea, M. I. Katsnelson, and A. K. Geim, *Nat. Phys.* **6**, 30 (2010).

<sup>48</sup>M. Vyshnepolsky *et al.*, *Appl. Phys. Lett.* **103**, 111909 (2013).

<sup>49</sup>H. D. Li *et al.*, *Appl. Phys. Lett.* **98**, 043104 (2011).

<sup>50</sup>Y. Liu *et al.*, *Nat. Phys.* **10**, 294 (2014).